

Article

Swelling and He-Embrittlement of Austenitic Stainless Steels and Ni-Alloys in Nuclear Reactors-Supplementary Material

Malcolm Griffiths ^{1,2,3,*}, Steven Xu ⁴ and Juan Eduardo Ramos Nervi ^{5,6}

² Dept of Mechanical & Aerospace Engineering, Carleton University, Ottawa, ON K1S 5B6, Canada

³ ANT International, 448 50 Tollered, Sweden

⁴ Kinectrics Inc., Toronto, ON M8Z 5G5, Canada; steven.xu@kinectrics.com

⁵ División de Materiales y Micromecánica, Gerencia de Ingeniería, Nucleoeléctrica Argentina S.A.; Francisco N. Laprida 3163, B1603AAA Villa Martelli, Argentina; jnervi@na-sa.com.ar

⁶ Centro Tecnológico Aeroespacial, Departamento de Aeronautica, Facultad de Ingeniería, Universidad Nacional de La Plata, Avda. 1 esq. 47, La Plata B1900TAG, Argentina

* Correspondence: malcolm.griffiths@queensu.ca

S1 Low Temperature He-Embrittlement

He-embrittlement has generally not been widely recognised as a low temperature (power reactor) phenomenon but, over the past 15-20 years, evidence has been accruing that inter-granular failure can occur due to He-embrittlement in reactor components at power-reactor operating temperatures (LWRs and HWRs). The characteristics of He-embrittlement are: (i) it is coincident with a decrease in the stresses and the strains at which failure occurs; (ii) it is inter-granular, Figure S1 [1].

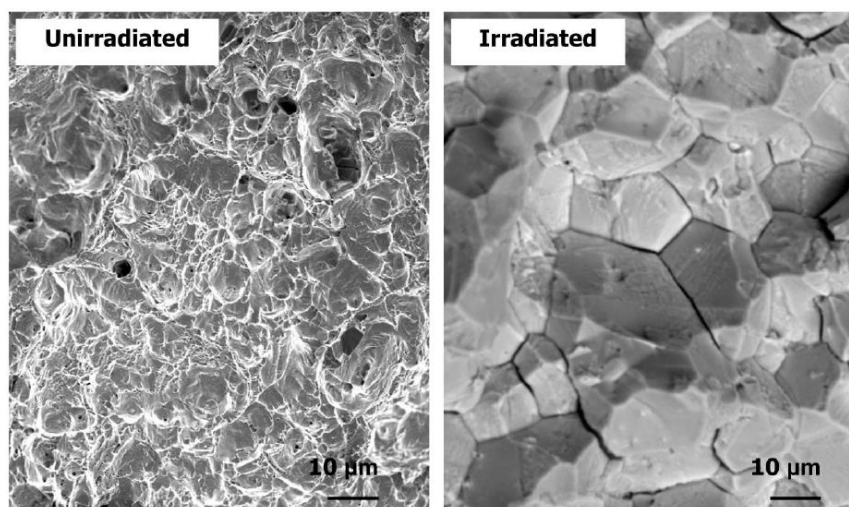


Figure S1. A comparison of fracture surfaces of Inconel X-750 spring material after crush testing to failure at room temperature. The unirradiated materials exhibits conventional ductile cup-cone fracture. The material irradiated in a CANDU reactor to dose of about 50 DPA at a nominal (estimated) temperature of 315 °C exhibits inter-granular failure.

Examinations of failed components indicate that the inter-granular failure is the result an excessive accumulation of cavities at grain boundaries for irradiation temperatures up to 350 °C [1]. Although the cavities are smaller at lower temperatures, which geometrically should lead to a higher area coverage per unit volume of cavity, detailed TEM measurements have shown that the coverage at a given dose increases as the temperature is increased and this is consistent with the lower failure loads for material irradiated at higher temperatures [2, 3]. There is considerable overlap in the area coverage measurements but, collectively, the tendency is to measure higher area coverage at higher

temperatures. A TEM micrograph showing cavities segregated on a boundary in irradiated Inconel X-750 is shown in Figure S2 [1].

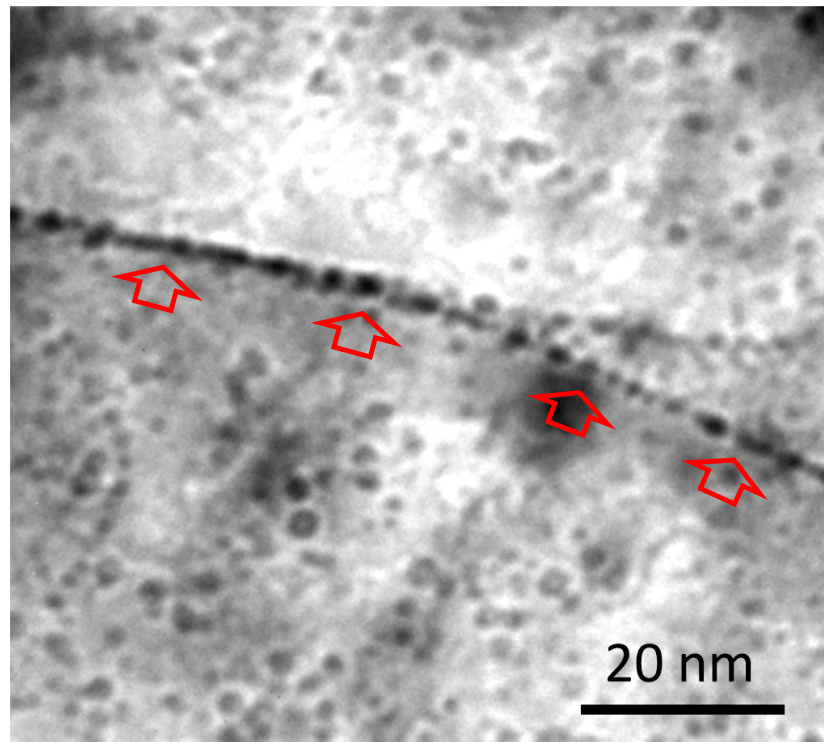


Figure S2. Over-focussed image showing cavities segregated on a grain boundary (arrowed) in Inconel X-750 after irradiation in a CANDU reactor to about 23 dpa at a temperature of about 315 °C.

Rate theory modelling shows that the grain boundary coverage increases at higher temperatures even though the cavities are larger and this is because of a larger net flux of vacancies and He atoms to the boundary as the temperature increases [2, 3]. The coverage is very much dependent on the grain interior microstructure as interactions with these internal sinks dictate how many point defects and He atoms migrate to the boundary. The concentration (area coverage) of cavities on the boundaries increases with increasing temperature; partly because the total sink strength in the grain interior is decreasing with increasing temperature allowing more point defects to migrate to the boundaries and partly because the He flux to the boundary is reduced by vacancy capture in the grain interior as the temperature is reduced. Because the vacancies are less mobile the steady-state concentration is elevated at low temperatures leading to more trapping of He atoms by single vacancies. The combined effect, shown by the model output, is that the coverage increases at higher temperatures within the bubble regime (<350 °C).

The relationship between grain boundary perforation and easy inter-granular fracture has also been demonstrated for 316 SS flux thimbles irradiated in a PWR. The work of Fujimoto et al. [4], Bosch et al. [5], and Edwards et al. [6, 7] showed that cavities were observed decorating grain boundaries in a 316 SS flux thimble irradiated in a PWR (Figure S3). They concluded that cavities at grain boundaries may promote IG failure and increase susceptibility to IGSCC. The irradiation-induced embrittlement observed for 316SS in a PWR after irradiation at 315°C to 70 dpa and 625 appm He is associated with grain boundary cavity segregation shown in the adjoining micrograph. The inter-granular fracture surface formed in the post-irradiation SCC test (Figure S3(a)) is indistinguishable from the fracture surfaces for similar material after post-irradiation tensile testing to failure in an inert atmosphere [4].

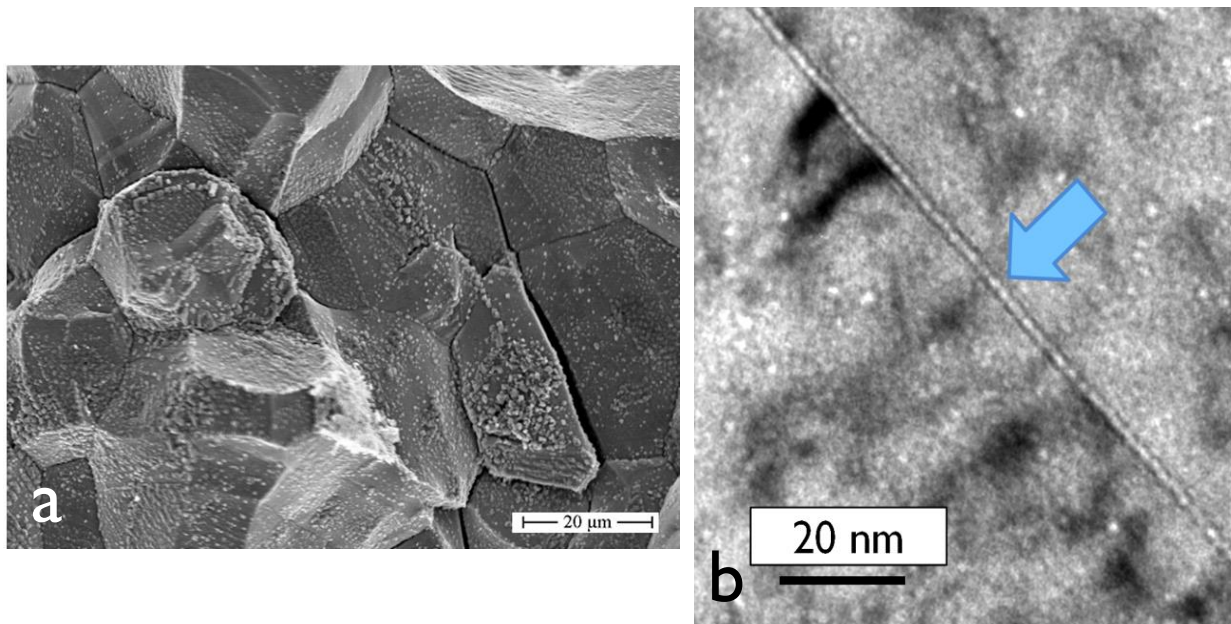


Figure S3. (a) Fracture surface showing inter-granular failure of 316 SS irradiated to 80 DPA at 320 °C and tested in PWR water chemistry at 55% of the irradiated yield, modified from [5]; and (b) TEM micrograph showing grain boundary cavity segregation in 316 SS irradiated in a PWR at 315 °C to 70 dpa and 625 appm He, modified from [6].

Similarly, Carsughi et al. [8] and James et al. [9] reported a transition to brittle inter-granular failure of Inconel 718 with increased dose for temperatures up to about 400 °C. Inconel 718 exhibited brittle inter-granular failure in the elastic regime after irradiation in the Los Alamos Neutron Science Center (LANSC) Accelerator Production of Tritium (APT) facility at a temperature of 367 °C - 400 °C, Figure S4 [9]. Carsughi et al. [8] stated that He embrittlement would be a possible explanation for their observations because He is generated by high energy protons. At 20 DPA the [He] concentration was estimated to be about 3000 appm [10]. Carsughi et al. [8] considered that the temperatures were too low for He-bubble segregation at grain boundaries and therefore another explanation was wanted, possibly the formation of a brittle phase at grain boundaries.

In view of more recent data on Inconel X-750 irradiated in CANDU reactors [2, 3], where [He] concentrations can be as high as 30,000 appm in a high power channel at EOL, He-stabilised cavities are a feasible explanation for He-embrittlement even though the temperatures likely range from 200 °C - 315 °C. Mass transport is a function of concentration and mobility (diffusion coefficient) so it is hardly surprising that embrittlement from He segregation at grain boundaries can occur at low temperatures when the [He] concentration is high as it is in HWRs.

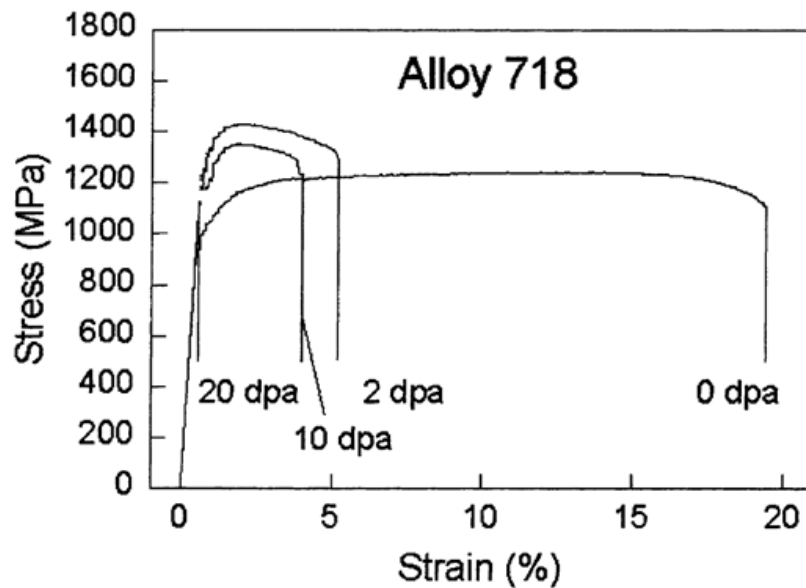


Figure S4. Room temperature stress-strain curves for Inconel 718 material extracted from the LANSCE window and irradiated at a temperature between 367 °C and 400 °C. Reproduced with permission from [9].

S2 High Temperature He-Embrittlement

At high temperatures He-embrittlement is a well-known phenomenon. Just as with the low temperature data, there is a direct correlation between the observation of cavities on boundaries and inter-granular failure. The most striking example of He-embrittlement has been demonstrated by Braski [11]. Braski showed that a V-15Cr-5Ti alloy irradiated to 17 DPA and 300 appm He at 550 °C exhibited brittle failure in the elastic regime (Figure S5). He showed that the low stress and strain at failure could be attributed to the segregation of He-stabilised cavities on grain boundaries (Figure S6). Although ferritic alloys are known to be embrittled at low temperatures (room temperature and below) they are not known for high temperature embrittlement except, as in this case, they also contain He. It is noteworthy there is little evidence of a high cavity density in the grain interior and the material tested by Braski therefore exhibited low swelling.

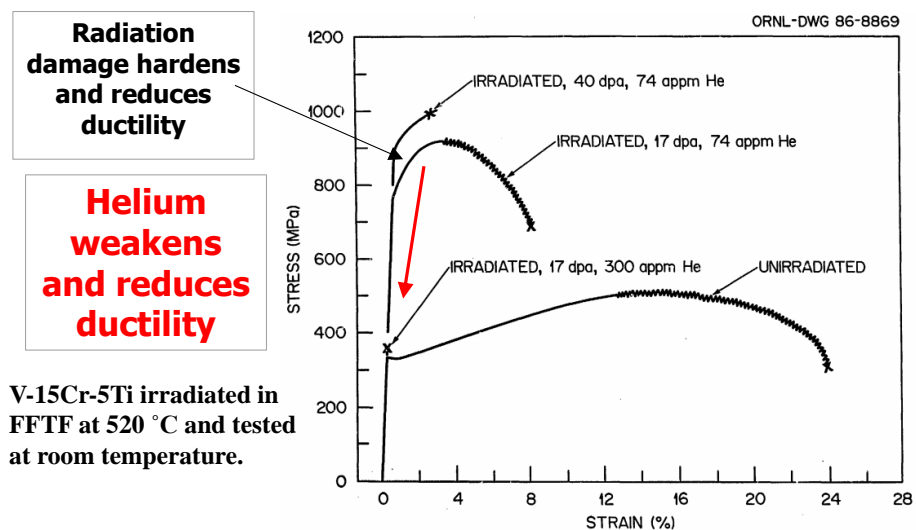


Figure S5. Room temperature stress-strain curves for ferritic V-15Cr-5Ti material irradiated in FFTF to various dose levels. Modified from [11].

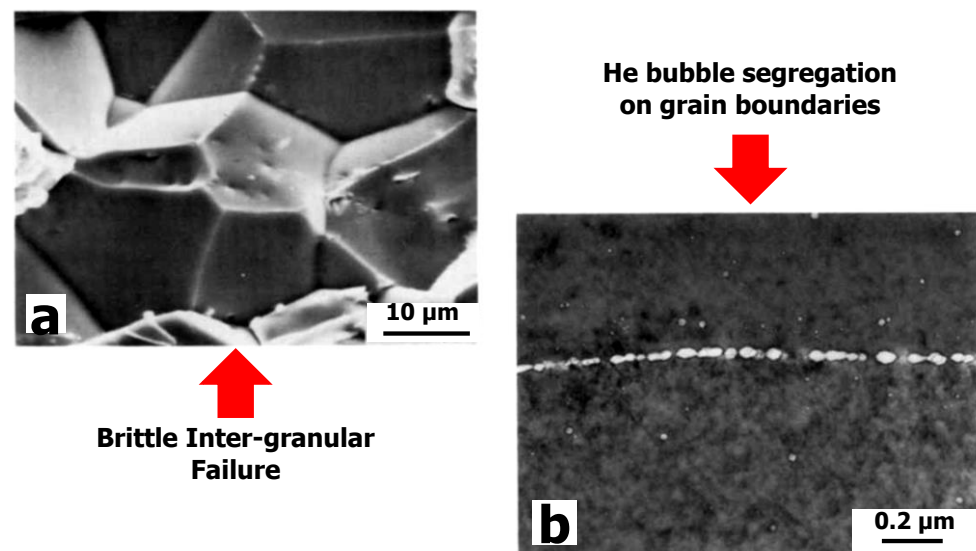


Figure S6. (a) Brittle intergranular fracture surface for a V-15Cr-5Ti specimen containing 300 appm He that was irradiated in FFTF to 17 dpa at 420°C and tested in tension at 420°C; (b) grain boundary bubbles in a V-15Cr-5Ti specimen with 74 appm He after irradiation in FFTF to 40 dpa at 520 °C. Modified from [11].

In general, one can say that He-embrittlement is not related to swelling, although high swelling may indicate the presence of He-stabilised cavities, but is very much dependent on segregation of He-stabilised cavities at grain boundaries.

The effect of He in promoting cavity segregation on boundaries is illustrated in Figure S7 [12,13]. Figure S7(a) is a TEM micrograph of a ferritic alloy (similar to that studied by Braski [11]) that was irradiated to high doses with self-ions. The material in (a) exhibited high swelling but there was no evidence of cavity segregation at boundaries. The converse is true for the Braski case (Figure S6(b)) and is also demonstrated for austenitic 316 SS irradiated with He ions, Figure S7(b). The commonality in all cases, whether neutron or ion irradiation, is that cavity segregation occurs at grain boundaries in the presence of He but not when He is absent.

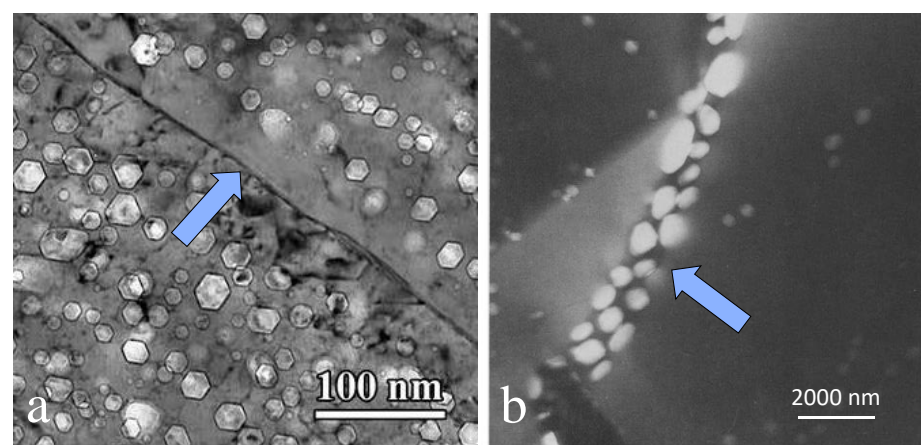


Figure S7. Voids in ion-irradiated materials: (a) Voids in MA957 ferritic alloy (Fe-14 wt%Cr, 0.9% Ti, 0.3% Mo) after Fe-ion irradiation to 500 dpa at 450°C – No He is produced and no grain boundary segregation, modified from [12]; (b) AISI 316 SS tested in tension to rupture at 1023K during He-ion irradiation; [He] = 2500 appm He: mean bubble diameter: 50 nm , modified from [13].

S3 Swelling-Induced Embrittlement

Swelling is often cited as being synonymous with embrittlement [14]. Swelling-induced embrittlement does not depend on cavity segregation at grain boundaries and is therefore not typically inter-granular in nature, although variations in the microstructure in the vicinity of grain boundaries may affect where failure occurs. The main characteristic of swelling-induced failure is the observation of classic cup and cone ductile dimples. These cup and cone features generally reflect micro-void formation and coalescence in a deformed material. Considering a tensile test specimen, rather than high (micro-void) porosity being present in the highly strained necked region of a tensile specimen prior to failure, a material that has a high void density is already porous and one is therefore closer to the failure point (in terms of porosity) when considering a standard mechanical test. The stress between the void ligaments is larger than the applied engineering stress, just as it is in a necked tensile specimen. If, for some reason, the deformation is localised due to inhomogeneities such as stringers, it is easy to see that failure can occur at lower stresses and strains than unperforated material and that swelling and embrittlement are synonymous.

Unlike He-embrittlement, where failure is restricted to the grain boundaries, swelling-induced embrittlement tends to be trans-granular with the fracture surface perpendicular to the tensile axis. Any association with grain boundaries can be ascribed to variations in the microstructure near the boundaries, for example, zones denuded of cavities near the boundary [12], Figure S7(a), or even depleted in precipitates and dislocation loops, all resulting in a softer region adjacent to the grain boundary. It therefore seems reasonable that the cup and cone failure associated with swelling-induced fracture may be more prevalent in, or adjacent to, regions where the material is softer.

An example of a fracture surface exhibiting localised cup and cone brittle failure is shown in Figure S8 [14].

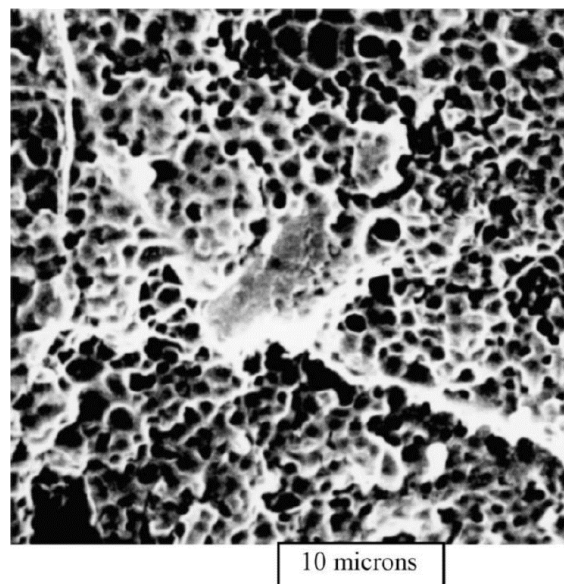


Figure S8. Fracture surface in an Fe-18Cr-10Ni-Ti austenitic stainless steel tensile specimen after testing at a swelling level of 30%. Modified from [14].

Neustroev and Garner [14] noted that material with high swelling values exhibited a trans-granular cup-cone morphology and thus failure proceeded by micropore coalescence arising from stress concentration between deforming voids. Similar fracture morphology has been observed in other studies on different stainless steels. They also reported that alloys containing 15 wt% Ni exhibited zero ductility at a lower dose than those with 10 wt% Ni. Although Neustroev and Garner [14] do not mention He production,

the higher Ni content will result in higher levels of He for a given dose, whether in a fast or thermal neutron environment, and one must consider the role that He could play in enhancing the embrittlement process.

Porollo et al. [15] described the fracture of Russian EI-847 stainless steel creep capsules tested to failure, which exhibited swelling levels in the BN-350 fast reactor of the order of 10% at temperatures of 335-365 °C and doses of 73-82 dpa. They noted the same cup and cone fracture attributed to swelling-induced embrittlement described by Neustroev and Garner [14], but also showed that the micro-void coalescence occurred preferentially at the edge of the denuded zones adjacent to grain boundaries, i.e. away from the boundary itself, see Figure S9. This unusual effect was attributed to the zone denuded of voids near the boundary. Being softer than the rest of the matrix it seems that the micro-void coalescence is easier in these regions and, as Porollo et al. state, the cracking then follows the grain boundaries without being on the grain boundaries.

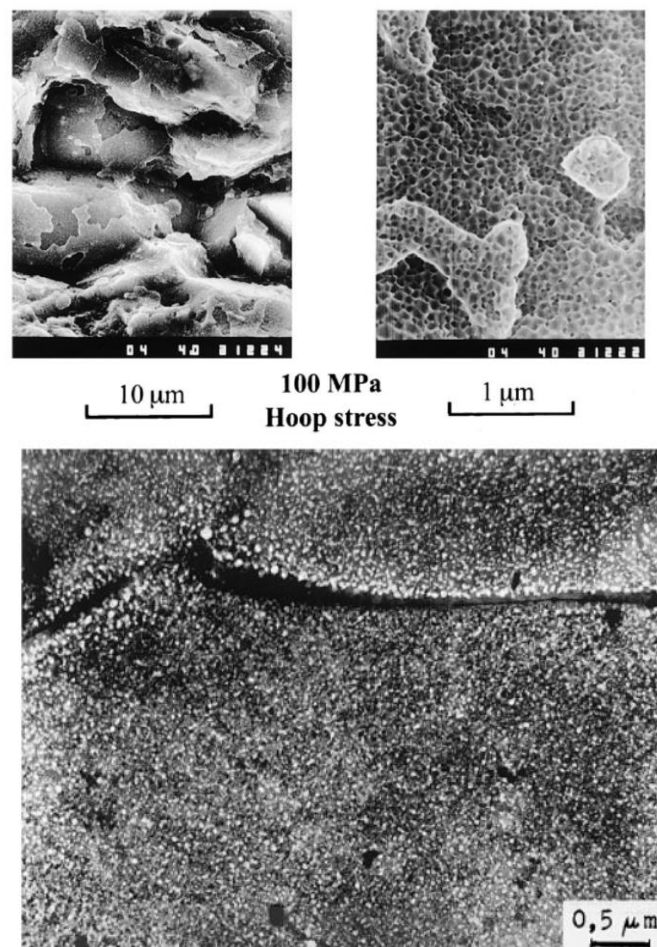


Figure S9. (a) Fracture surface of failed cold-worked creep tube at 365°C and 83 dpa, showing ductile coalescence of voids parallel to grain boundaries; (b) Large voids associated with cracking along denuded zone adjacent to grain boundaries at 335°C and 73 dpa in an annealed stress-free tube. Modified from [15].

Although there are cases where cracking is observed in a high swelling material by the inter-linking between uniformly distributed voids, such a mechanism should not be confused with He-embrittlement, which occurs preferentially at grain boundaries because there is a higher density of cavities on the boundary compared with the matrix.

He-embrittlement is characterised by inter-granular failure and is considered a high temperature phenomenon. One might consider that cavity segregation will be more pronounced at high temperatures if there is also higher swelling because it is an indication of

higher He/DPA levels [16]. For low He/DPA values, the swelling in a PWR or fast reactor such as EBR-2 decreases at higher temperatures, but the lower sink strength in the grain interior also results in more cavities on the boundary, i.e. more He embrittlement when the void swelling is low. Therefore, He-embrittlement may be prominent even when there is low swelling. An example of material with low swelling but having a high density of He-stabilised cavities on the grain boundary is shown in Figure S6.

S4 Trans-Granular Failure

Whereas swelling-induced embrittlement can be described as involving an intra-granular cracking process, the occasional observations of trans-granular failure in materials exhibiting He embrittlement may be unrelated. Citing Hamilton et al. [17], Neustroev and Garner [14] state that, “segregation of nickel to void surfaces causes martensitic instability in the matrix, especially at the crack tip. This in turn produces a tearing modulus of zero and transgranular failure with the failure surface completely coated with alpha martensite.”

These claims are based on the interpretation of one unidentified reflection with a diffracting vector consistent with the BCC phase and used to create a dark-field image from a TEM sample taken at the fracture surface [17]. The area corresponding with the diffraction pattern is not specified and the pattern itself is indexed as if it is a $\langle 111 \rangle$ pole but does not exhibit six-fold symmetry. Whereas the claim that the phase is BCC may be correct, for other reasons, the proof has not been provided. Rather than forming α - or even α' -martensite at the fracture surface it is possible that cracking occurs along an existing platelet phase. Given that Hamilton et al. [17] also refer to ϵ -martensite and twin platelets in the base unirradiated material, it is conceivable that the phase identified on the surface fracture is comprised of ϵ -martensite or twin platelets and is present prior to irradiation.

The interfaces between hexagonal-close-packed (HCP) platelets (η -phase) and the face-centred-cubic (FCC) matrix have been identified as preferential sites for cracking in PE-16 [18]. It begs the question whether the fracture surface noted by Hamilton et al. [17] could be ϵ -martensite or a twin/ ϵ -martensite complex. Such platelet structures are often observed in stainless steels after cold-working [16]. To support this notion trans-granular platelets decorated with He-stabilised cavities have been observed in neutron irradiated Inconel X-750 [19], Figure S10.

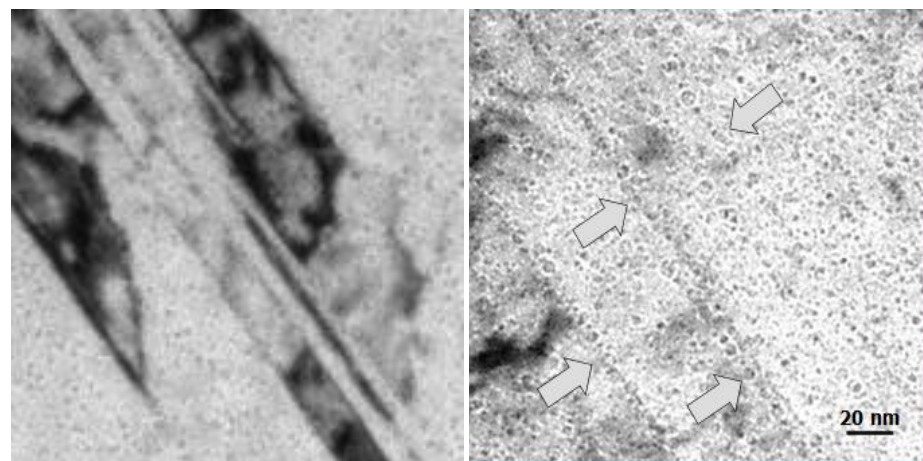


Figure S10. TEM micrographs of Inconel X-750 material irradiated to ~ 55 dpa, ~ 18000 appm He at about 315 °C, showing planar sub-grain boundaries (possibly incoherent twins or ϵ -martensite platelets) covered with helium bubbles (arrowed). Modified from [19].

Whereas irradiation-enhanced embrittlement may be the result of matrix hardening and the incompatibility with the platelet phases, it is also conceivable that an increase in

cavity segregation on these platelets may contribute to the preferential fracture at these locations. He is especially important because it not only enhances cavity growth but also stabilises cavities on grain and other interface boundaries [20].

S5 He-Embrittlement and IASCC

The stress corrosion cracking (SCC) and irradiation assisted stress corrosion cracking (IASCC) susceptibility of austenitic alloys such as stainless steels and other Ni-alloys has been the subject of great concern to the nuclear industry. Cracking is often inter-granular in nature and depends on the combined effects of stress, the environment and the material [21]. SCC and IASCC tests are slow strain rate tests generally conducted below the yield stress, like a creep ductility test. They are distinguished from creep ductility tests by adding the environmental factor. In the case of fracture toughness, the applied engineering stress may be below the engineering yield stress while the stress at the crack is above the yield stress thus generating crack advance in a ductile manner. Normally crack-blunting may be expected to arrest crack advance. Crack advance can progress, however, by corrosion creating new sharp cracks. Fracture toughness or creep ductility tests conducted in an inert corrosion environment provide information about the mechanical properties (embrittlement for example) that cannot be assigned to an SCC or IASCC process. For irradiated materials, characterising the susceptibility of material changes caused by irradiation to an IASCC mechanism cannot be performed with a single test because one does not know whether the changes to the material are simply affecting the creep ductility or fracture toughness and a control test in an inert environment is required.

When grain boundaries are embrittled by He, this may affect the interpretation of IASCC effects. At the same time the segregation of He at grain boundaries must be considered when interpreting changes in the chemistry, Cr depletion in particular, at grain boundaries that is widely viewed as detrimental to IASCC. In 2005, when Edwards et al. [6] reported that He bubbles are present on grain boundaries in 316 SS irradiated in a PWR, it was widely viewed as a milestone in improved understanding of the behaviour of stainless steels in a power reactor environment. The observation of Edwards et al. begs the question whether work conducted prior to 2005 could be re-interpreted, bearing in mind that He bubbles can be expected to be present on boundaries for similarly irradiated materials. One example is the work of Bruemmer et al. published in 1999 [22]. They showed that Cr was depleted at grain boundaries as a result of irradiation, Figure S11 [22]. Apart from the embrittling effect of perforated grain boundaries, if He bubbles were also present on the boundary (arrowed in Figure S11) they will be preferential vacancy sinks thus supporting the notion that the Cr depletion is the result of inverse-Kirkendall diffusion. Preferential Cr depletion at the boundary is the result of the vacancy flux to the boundary because Cr atoms are faster self-diffusers compared with the other elements present [23]. Whereas one might expect an excess flux of vacancies to grain boundaries because interstitials are absorbed at biased dislocation sinks within the grain interior, the existence of He bubbles on the boundary will also provide an additional driving force for a vacancy flux because the bubbles will preferentially absorb vacancies compared with interstitials, irrespective of irradiation, if the temperature is high enough and vacancies are mobile. Bubbles that are 1-2 nm in diameter may not be easily imaged in an electron microscope unless the objective lens stigmators are well-aligned (irrespective of the degree of Fresnel focus) so one may suspect that such small bubbles may not have been noticed until Edwards et al. [6] showed their existence.

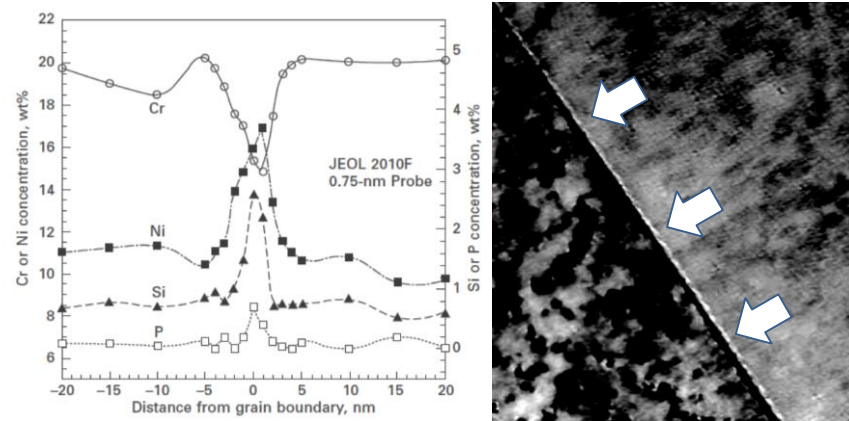


Figure S11. Composition profiles across a grain boundary in a neutron-irradiated 300-series stainless steel and corresponding TEM image with boundary. Modified from [22].

He bubbles on boundaries are not the only driving force for Cr depletion. In other work, Andresen and Was [24] showed how the concentration of Cr on the boundary of various austenitic stainless steels decreases with increasing dose, Figure S12 [24].

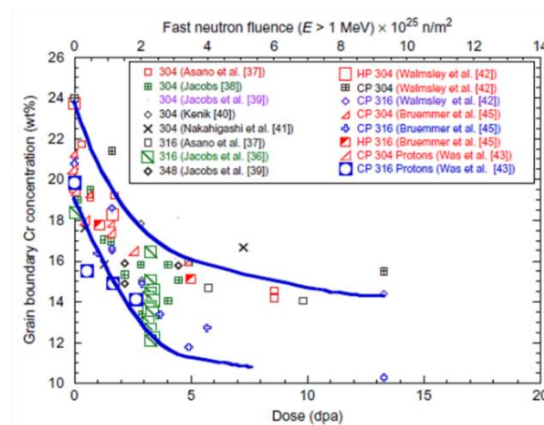


Figure S12. Dose dependence of grain boundary chromium concentration for several 300-series austenitic stainless steels irradiated at temperatures about 300 °C. Reproduced with permission from [24].

Although the Cr depletion at grain boundaries has been called a radiation-induced effect, radiation-enhanced diffusion due to an elevated vacancy concentration also provides a mechanism to explain the chemical redistribution that occurs. The effect of irradiation in the range of temperatures relevant to operation in a PWR (300 °C – 350 °C) is to enhance the self-diffusion coefficient to levels that are the same as if the temperature was about 550 °C [1, 16]. For an alloy that has not been de-sensitised to Cr depletion by precipitating all the available carbon by heat treatment, it is reasonable to expect some Cr-carbide precipitation after about 3-4 years of operation in a PWR simply because of the radiation-enhanced self-diffusion. The radiation enhancement of self-diffusion will be larger as the dose rate is increased in the case of ion irradiation and the effective temperature will be correspondingly higher, even though the irradiation time may be less. An indication that Cr depletion during ion irradiation is linked with carbide precipitation comes from the work of Fournier et al. [25]. They examined the effect of adding Pt and Hf on the RIS at grain boundaries in austenitic stainless steels using proton irradiation. They noted a “spectacular” effect of Hf in suppressing the depletion of Cr at grain boundaries. If the depletion of Cr is the result of radiation-enhanced diffusion and carbide formation, then the effect of adding Hf in reducing Cr depletion may be understood because it is a carbide former. The presence of Hf, which will react with any excess carbon, is one

way to reduce Cr-carbide formation and thus limit the amount of apparent depletion of Cr at grain boundaries that is otherwise attributed to RIS.

Supplemental References

- Griffiths, M. The Effect of Irradiation on Ni-containing Components in CANDU Reactor Cores: A Review. *AECL Nucl. Rev.*, **2013**, 2, 1–16; erratum *AECL Nucl. Rev.* **2014**, 3,89.
- Judge, C.D.; Rajakumar, H.; Korinek, A.; Botton, G.; Cole, J.; Madden, J.W.; Jackson, J.H.; Freyer, P.D.; A, L.; Giannuzzi; Griffiths, M. High Resolution Transmission Electron Microscopy of Irradiation Damage in Inconel X-750. In *Proceedings of the 18th International Conference on Environmental Degradation of Materials in Nuclear Power Systems–Water Reactors*; Portland WA August 13–17, 2017, The Minerals, Metals & Materials Series; Springer: Cham, Switzerland, 2018. https://doi.org/10.1007/978-3-319-67244-1_47.
- Xu, S.X.; Griffiths, M.; Scarth, D.A.; Graham, D. Microstructure-based Polycrystalline Finite Element Modeling of Inconel X-750 Irradiated in a CANDU Reactor, Accepted for publication in *Engineering Fracture Mechanics*, Special Issue on Progress and Issues of Fracture in Pressure Vessels and Piping (2022).
- Fujimoto, K.; Yonezawa, T.; Wachi, E.; Yamaguchi, Y.; Nakano, M.; Shogan, R.P.; Massoud, J.P.; Mager, T.R. Effect of the accelerated irradiation and hydrogen/helium gas on IASCC characteristics for highly irradiated austenitic stainless steels, In *Proceedings of 12th International Conference on Environmental Degradation of Materials in Nuclear Power System – Water Reactors*, Salt Lake City, Utah, 14–18 August 2005; 299–310.
- Bosch, R.W.; Vankeerberghen, M.; Gérard, R.; Somville, F. Crack initiation testing of thimble tube material under PWR conditions to determine a stress threshold for IASCC, *J. Nucl. Mater.* **2015**, 461, 112–121.
- Edwards, D.J.; Simonen, E.P.; Bruemmer, S.M.; Efsing, P. Microstructural evolution in neutron-irradiated stainless steels: comparison of LWR and fast-reactor irradiations. In *Proceedings of 12th International Conference on Environmental Degradation of Materials in Nuclear Power System—Water Reactors*, Salt Lake City, Utah, 14–18 August 2005; 419–428.
- Edwards, D.J.; Garner, F.A.; Bruemmer, S.M.; Efsing, P. Nano-cavities observed in a 316 SS PWR flux thimble tube irradiated to 33 and 70 dpa, *J. Nucl. Mater.* **2009**, 384, 249–255.
- Carsughi, F.; Derz, H.; Pott, G.; Sommer, W.; Ullmaier, H. Investigations on Inconel 718 Irradiated with 800 MeV Protons, *J. Nucl. Mater.* **1999**, 264, 78–88.
- James, M.R.; Maloy, S.A.; Gac, F.D.; Sommer, W.F.; Chen, J.; Ullmaier, H. The mechanical Properties of an Alloy 718 Window after Irradiation in a Spallation Environment, *J. Nucl. Mater.* **2001**, 296, 139–144.
- Griffiths, M. Ni-based Alloys for Reactor Internals and Steam Generator Applications, chapter 9. In *Structural Alloys for Nuclear Energy Applications*; Zinkle, S., Odette, R., Eds.; Elsevier: Amsterdam, The Netherlands; ISBN 9780123970466 (2019).
- Braski D.N. The effect of neutron irradiation on vanadium alloys, *J. Nucl. Mater.* **1986**, 141–143, 1125–1131.
- Toloczko, M.B.; Garner, F.A.; Voyevodin, V.N.; Bryk, V.V.; Borodin, O.V.; Melnychenko, V.V.; Kalchenko, A.S. Ion-Induced Swelling of ODS Ferritic Alloy MA957 Tubing to 500 dpa, *J. Nucl. Mater.* **2014**, 453, 323–333.
- Schroeder, H.; Batfalsky, P. The dependence of the high temperature mechanical properties of austenitic stainless steels on implanted helium. *J. Nucl. Mater.* **1983**, 115, 297–306.
- Neustroev, V.S.; Garner, F.A. Severe embrittlement of neutron irradiated austenitic steels arising from high void swelling, *J. Nucl. Mater.* **2009**, 386–388, 157–160.
- Porollo, S.I.; Vorobjev, A.N.; Konobeev, Yu.V.; Dvoriashin, A.M.; Krigan, V.M.; Budylnin, N.I.; Mironova, E.G.; Garner, F.A. Swelling and void-induced embrittlement of austenitic stainless steel irradiated to 73–82 dpa at 335–365°C, *J. Nucl. Mater.* **1998**, 258–263, 1613–1617.
- Griffiths, M. Effect of Neutron Irradiation on the Mechanical Properties, Swelling and Creep of Austenitic Stainless Steels. *Materials* **2021**, 14, 2622.
- Hamilton, M.L.; Huang, F.H.; Yang, W.J.; Garner, F.A. Mechanical properties and fracture behavior of 20% cold-worked 316 stainless steel irradiated to very high neutron exposures. In: *Influence of Radiation on Material Properties: 13th International Symposium (Part II)*, ASTM International: West Conshohocken, PA, USA, 1987. pp. 245–270.
- Rowcliffe, A.F.; Mansur, L.K.; Hoelzer, D.T.; Nanstad, R.K. Perspectives on Radiation Effects in Nickel-Base Alloys For Applications In Advanced Reactors. *J. Nucl. Mater.* **2009**, 392, 341–352.
- Judge, C.D. PhD Thesis, The Effects of Irradiation on Inconel X-750, McMaster University, November 2015. Available online: <https://macsphere.mcmaster.ca/handle/11375/18091> (accessed on Sept 9 2022).
- Griffiths, M.; Boothby, R. Radiation Effects in Nickel-Based Alloys. In *Reference Module in Materials Science and Materials Engineering*; Comprehensive Nuclear Materials; Konings, R., Ed.; Elsevier: Amsterdam, The Netherlands, 2020; pp. 334–371.
- Was, G. S.; Busby, J.; Andresen, P.L. Effect of Irradiation on Stress Corrosion Cracking and Corrosion in Light Water Reactors; in “*ASM Handbook on Corrosion; Environments and Industries*”, Vol. 13C, **2006**, 386–414.

-
22. Bruemmer, S.M.; Simonen, E.P.; Scott, P.M.; Andresen, P.L.; Was, G.S.; Nelson, J.L. Radiation-induced material changes and susceptibility to intergranular failure of light-water-reactor core internals, *J. Nucl. Mater.* **1999**, *274*, 299–314.
 23. Zhao, S.; Egami, T.; Stocks, G.M.; Zhang, Y. Effect of d electrons on defect properties in NiCoCr and NiCoFeCr concentrated solid solution alloys, *Phys. Rev. Mater.* **2018**, *013602*, 1–18. <https://doi.org/10.1103/PhysRevMaterials.2.013602>.
 24. Andresen, P.L.; Was, G.S. Irradiation Assisted Stress Corrosion Cracking, *Comprehensive Nuclear Materials (Second Edition)*, Editor(s): Rudy J.M. Konings, Roger E. Stoller, Elsevier, **2019**, *4.07*, 190–217.
 25. Fournier, L.; Sencer, B.L.; Was, G.S.; Simonen, E.P.; Bruemmer, S.M. The influence of oversized solute additions on radiation-induced changes and post-irradiation intergranular stress corrosion cracking behavior in high-purity 316 stainless steels, *J. Nucl. Mater.* **2003**, *321*, 192–209.